Journal of Physics: Conference Series **428** (2013) 012015 doi:10.1088/1742-6596/428/1/012015

Jahn-Teller theory beyond the standard model

S Bhattacharyya[1], D Opalka[1,3], L V Poluyanov[2] and W Domcke[1]

[1] Department of Chemistry, Technische Universität München, D-85747 Garching, Germany
[2] Institute of Chemical Physics, Academy of Sciences, Chernogolovka, Moscow 142432, Russia

E-mail: swarnendu.bhattacharyya@ch.tum.de, domcke@ch.tum.de

Abstract. In the standard model of Jahn-Teller (JT) theory, the spin-free electronic Hamiltonian is expanded up to second order in normal-mode displacements, while the spin-orbit (SO) coupling operator is approximated in zeroth order. In this article, the systematic extension of JT theory beyond the standard model is outlined. For the classic $E \times e$ and $T_2 \times t_2$ JT problems in C_{3v} and T_d symmetry, respectively, it is shown how the conventional Taylor expansion of the spin-free Hamiltonian can be replaced by an expansion in invariant polynomials up to arbitrarily high orders. The theory of SO coupling in JT systems is extended beyond the standard model by an expansion of the Breit-Pauli SO-coupling operator up to first order in normal-mode displacements. The spectroscopic relevance of the higher-order electrostatic and the linear relativistic JT coupling terms is illustrated for the vibronic structures of the photoelectron spectra of tetrahedral P_4 and Sb_4.

1. Introduction

The theory of vibronic coupling, which includes Jahn-Teller (JT) theory [1] and Renner theory [2] as special cases, is based on the following concepts :

(i) Representation of the electronic Hamiltonian in a basis of diabatic [3] electronic states.
(ii) Expansion of the electronic Hamiltonian in a Taylor series at the reference geometry of high symmetry.
(iii) Use of symmetry selection rules to determine the non-vanishing matrix elements.

In the "standard model" of JT theory, which is described in numerous reviews, monographs and edited volumes on the JT effect [4–11], the electrostatic (spin-free) Hamiltonian is expanded up to second order in normal-mode displacements. The spin-orbit (SO) coupling operator, which becomes relevant for systems containing heavier elements (e.g. transition metals, lanthanides or actinides) is approximated at zeroth order, that is, at the high-symmetry reference geometry [4–11].

Extensions of the electrostatic JT Hamiltonian beyond the standard model were occasionally considered for specific systems. For example, the third-order and fourth-order terms in the $E \times e$ Hamiltonian [12] for trigonal systems have been included in some investigations of static and dynamic JT effects in clusters and solids [13–16]. The systematic expansion of the electrostatic $E \times e$ JT Hamiltonian for trigonal systems up to sixth order has first been given by Viel and Eisfeld [17]. Applications of such high-order $E \times e$ Hamiltonians have been reported, for

[3] Present address: Department of Chemistry, University of Cambridge, Cambridge CB2 1EW, UK

example, for the methoxy and NO_3 radicals [18, 19], the ammonia cation [20] and transition-metal trifluorides [21]. It was discovered by *ab initio* calculations that "intramolecular collisions" of the ligand atoms at large amplitudes of the JT-active bending mode result in a pronounced positive anharmonicity of the *ab initio* bending potentials, which requires a JT expansion up to at least sixth-order in the bending mode [21, 22].

A general symmetry-adapted polynomial expansion of electrostatic $T \times t$ and $T \times e$ JT Hamiltonians in tetrahedral systems has been developed by Opalka and Domcke [23, 24]. This approach combines JT theory with the theory of invariant polynomials [25]. Symmetry-adapted polynomials up to high orders were explicitly given and a combinatorial scheme was developed to express terms of arbitrary order as products of a small number of invariant polynomials. The method was applied to the methane cation in its triply degenerate ($^2T_2$) ground state. Terms up to 12th order in the t_2 bending mode, up to 8th order in t_2 stretching mode and up to 10th order in the bending mode of e symmetry were included. The parameters were determined by a nonlinear least-squares fitting of a large set of *ab initio* data obtained at the full-valence CASSCF/MRCI/cc-pVTZ level [23, 24].

In the vast literature on the JT effect in solids, the SO coupling operator has been approximated by an effective atom-like SO operator, which, as such, is independent of the nuclear coordinates [4–7]. In treatments of joint JT and SO couplings in molecules, the SO splitting likewise was taken as independent of the nuclear coordinates and approximated by its value at the high-symmetry reference geometry [8–10]. A theoretical description of the SO coupling beyond the standard model has been developed only recently in the work by Poluyanov and Domcke for the trigonal, tetragonal, tetrahedral and cubic point groups [26–30]. In this approach, the SO interaction is considered as a perturbation of the electrostatic electronic Hamiltonian $\mathcal{H}_{el}$,

$$\mathcal{H}_{el} = \mathcal{H}_{es} + \mathcal{H}_{SO} \tag{1}$$

where $\mathcal{H}_{SO}$ is the Breit-Pauli SO operator [31]. The latter can be derived from the Dirac-Coulomb-Breit operator either by the elimination of the small components or by a perturbation expansion in c^{-1} [32]. A nonrelativistic spin-orbital electronic basis is employed and the Breit-Pauli operator is treated exactly as in the nonrelativistic vibronic coupling theory, that is,

(i) Representation of the Breit-Pauli operator in a basis of (nonrelativistic) diabatic [3] electronic states.

(ii) Expansion of the Breit-Pauli operator in powers of normal-mode displacements at the reference geometry.

(iii) Use of symmetry selection rules to determine the nonvanishing matrix elements.

Assuming that the SO coupling is a relatively weak perturbation of the electrostatic Hamiltonian, the Taylor expansion of the SO operator was terminated at first order. This way, the relativistic JT forces (arising from the SO operator) are included in the JT Hamiltonian. The existence of relativistic JT forces was revealed for the tetragonal, tetrahedral and cubic point groups [27–30]. In trigonal systems, on the other hand, the linear relativistic JT coupling constants are zero by symmetry [26].

In this article, we give a synopsis of recent theoretical developments which extend the JT theory systematically beyond the standard model. The motivation for these developments arises primarily from modern quantum chemistry. In order to harness the phenomenal progress in *ab initio* electronic-structure theory, including relativistic quantum chemistry, it is a necessity to develop JT theory substantially beyond the standard model. The latter was conceived during the 1940s and 1950s, at a time when the JT and SO coupling parameters had to be determined via the fitting of at best a few low-resolution spectral data, which required that the number of adjustable parameters had to be kept to a minimum. Nowadays, an essentially unlimited

amount of data can be generated by accurate *ab initio* electronic-structure calculations, which eliminates the restriction of JT and SO coupling Hamiltonians to low-order expansion terms with just few coupling parameters.

2. Expansion of the spin-free Jahn-Teller Hamiltonian beyond second order

2.1. Polynomial invariant theory and Jahn-Teller Hamiltonian

The potential-energy (PE) surfaces of polyatomic molecules containing N identical nuclei are subject to permutational invariance of like nuclei. The permutations of the identical nuclei in a molecule form a group, the so-called Complete Nuclear Permutation (CNP) group which is nothing but the symmetry group of N identical nuclei (S_N) [33, 34]. Being a proper subgroup of the full symmetry group of the molecular system, the elements of the CNP group commute with the Hamiltonian. The molecular point group, on the other hand, is defined (locally) if a well-defined equilibrium geometry exists in a certain region of the PE surface. In recent years, the exploitation of permutation symmetry has been of increasing interest in the construction of analytic representations of global PE surfaces. Polynomials, invariant in the CNP group, have been employed to form a set of invariant functions which provide an approximation space for analytic PE surfaces [35].

The established description of the JT effect relies on the symmetry of the irreducible representations of the molecular point group defined at the configuration of highest symmetry. It will be shown below that in many cases of interest the irreducible representations of the molecular point group (matrix groups) are isomorphic to those of the permutation symmetry group. Therefore, the methods of invariant theory [25] can be employed for the efficient derivation of JT Hamiltonians.

The invariance of a polynomial under a linear algebraic group G can be defined as follows

$$\sigma \circ p(\mathbf{v}) = p(\sigma^{-1}\mathbf{v}) = p(\mathbf{v}) \tag{2}$$

where σ is a matrix representation of all the elements in G, p is an element of the ring of invariant polynomials under the group G ($\mathbb{K}[V]^G$) and $\mathbf{v}$ is an element of the underlying vector space V. The evaluation of the group action on the polynomials requires the matrix representations of the elements of the group. The generating set of invariant polynomials under the action of a finite linear group G can be obtained by the successive application of the Reynolds operator (which is a G-invariant projection) to all terms of a general polynomial expansion

$$\mathcal{R}(p) = \frac{1}{|G|}\sum_{\sigma\in G}\sigma \circ p. \tag{3}$$

Hilbert has given the proof (Hilbert's finiteness theorem) [36] that the ring of invariant polynomials $\mathbb{K}[V]^G$ under the group G is finitely generated by the generating set of homogeneous invariant polynomials $(p_1, \ldots, p_r)$ which is a subset of $\mathbb{K}[V]^G$, i.e.

$$\mathbb{K}[V]^G = \mathbb{K}[p_1, \cdots, p_r]. \tag{4}$$

The generating set of invariant polynomials has an *a priori* upper bound of their degree which is given by the order of the group $|G|$ (Noether degree bound) [37].

The linearly independent elements of $\mathbb{K}[p_1, \cdots, p_r]$ form a vector space and the adiabatic PE surface can be approximated by restricting the expansion up to a certain order. In the case of a single PE surface, defined by $\langle\boldsymbol{\varphi}|\mathcal{H}_{el}|\boldsymbol{\varphi}\rangle$, where $|\boldsymbol{\varphi}\rangle$ is an adiabatic electronic state, the Hamiltonian $\mathcal{H}_{el}$ is a totally symmetric function of nuclear coordinates and the electronic wave function $|\boldsymbol{\varphi}\rangle$ is invariant under symmetry operations. Multi-sheeted intersecting adiabatic PE surfaces, on the other hand, cannot be approximated by polynomial expansions due to the

presence of cusps at conical intersections. Therefore, a representation of the multi-sheeted PE surface in a diabatic basis must be found to express the elements of the diabatic PE matrix as smooth functions of the nuclear coordinates.

The adiabatic electronic wave functions of a manifold of m intersecting electronic PE surfaces can be represented as superpositions in an m-dimensional diabatic basis, which forms an electronic sub-Hilbert space. Assuming that all other electronic states are sufficiently far apart in energy, the wave function is written as

$$|\mathbf{\Psi}\rangle = \sum_{i=1}^{n} c_i |\boldsymbol{\varphi}_i^d\rangle \tag{5}$$

where the $|\boldsymbol{\varphi}_i^d\rangle$ are diabatic [3, 38–40] electronic basis states. The expectation value of the electronic Hamiltonian can be expressed as a function of nuclear coordinates and electronic coefficients

$$\begin{aligned} \langle \mathcal{H}_{el} \rangle &= \langle \mathbf{\Psi} | \mathcal{H}_{el} | \mathbf{\Psi} \rangle \\ &= \sum_{i,j} c_i \langle \boldsymbol{\varphi}_i^d | \mathcal{H}_{el} | \boldsymbol{\varphi}_j^d \rangle c_j \\ &= \sum_{i,j} c_i (\mathcal{H}_{el})_{ij} c_j . \end{aligned} \tag{6}$$

The energy expectation value (6) is quadratic in the electronic coefficients and $\mathcal{H}_{el}$ is expanded in terms of polynomials in symmetry-adapted nuclear coordinates. Therefore, we have to find the second-order invariants in the vector space V^{el} and the invariant polynomials in the vector space V^{nu} of the symmetry-adapted nuclear coordinates.

The most transparent case arises when the nuclear and the electronic basis functions transform according to the same irreducible representation, such as in the $E \times e$ and $T_2 \times t_2$ JT effects. In this case, the nuclear coordinates and electronic states form identical vector spaces and their matrix group representations are also identical in both coordinate spaces ($\Gamma^{el} = \Gamma^{nu}$). Weyl's polarization method can then be used to obtain the generating polynomials from the generators of the invariant ring of a single copy of these [41, 42]. The JT vibronic matrix can then very efficiently be constructed as the Hessian (with respect to the electronic degrees of freedom) of the invariant polynomials [23, 24].

2.2. The E×e Jahn-Teller Hamiltonian

Molecules of C_{3v} symmetry possess degenerate electronic states of E symmetry and degenerate vibrational modes of e symmetry [12], which transform like x, y in the C_{3v} point group. The polynomial invariants of the E representation in C_{3v} form a ring and are finitely generated by two polynomials of degree 2 and 3 respectively, which form the so-called generating set of the invariant ring. These are [42]

$$\begin{aligned} f_1 &= x^2 + y^2 \\ f_2 &= x^3 - 3xy^2 . \end{aligned} \tag{7}$$

All the elements of the ring $\mathbb{K}[x, y]^{C_{3v}}$ can be constructed in terms of these generators

$$\mathbb{K}[x, y]^{C_{3v}} = \mathbb{K}[f_1, f_2]. \tag{8}$$

The ring of the C_{3v}-invariant polynomials in the direct sum of two vector spaces of E symmetry (electrons) and e symmetry (nuclei), $\mathbb{K}[V^E \oplus V^e]^{C_{3v}}$ can be computed from

$\mathbb{K}[V^e]^{C_{3v}} = \mathbb{K}[f_1, f_2]$ by Weyl's polarization method [41]. As Weyl's polarization operator is a linear differential operator, the JT matrix expansion of any order n can be found by taking the Hessian of all possible products of the primary invariants of order $(n+2)$. After eliminating the redundant terms, it is straightforward to represent the $E \times e$ JT expansion of any order as a sum of the trace and a traceless matrix [17]

$$\mathcal{H}_{es}^{(n)}[E \times e] = \begin{pmatrix} \mathcal{V}^{(n)} & 0 \\ 0 & \mathcal{V}^{(n)} \end{pmatrix} + \begin{pmatrix} \mathcal{W}^{(n)} & \mathcal{Z}^{(n)} \\ \mathcal{Z}^{(n)} & -\mathcal{W}^{(n)} \end{pmatrix}. \tag{9}$$

The well-known first-order and second-order JT Hamiltonians are the Hessians of f_2 and f_1^2 respectively.

The expansion of the $E \times e$ JT Hamiltonian up to sixth order is given by

$$\begin{aligned}
\mathcal{V}^{(1)} &= 0 \\
\mathcal{V}^{(2)} &= a_1^{(2)}(x^2 + y^2) \\
\mathcal{V}^{(3)} &= a_1^{(3)}(x^3 - 3xy^2) \\
\mathcal{V}^{(4)} &= a_1^{(4)}(x^4 + 2x^2y^2 + y^4) \\
\mathcal{V}^{(5)} &= a_1^{(5)}(x^5 - 2x^3y^2 - 3xy^4) \\
\mathcal{V}^{(6)} &= a_1^{(6)}(x^6 + 3x^4y^2 + 3x^2y^4 + y^6) + a_2^{(6)}(x^6 - 6x^4y^2 + 9x^2y^4)
\end{aligned} \tag{10}$$

$$\begin{aligned}
\mathcal{W}^{(1)} &= \lambda_1^{(1)}x \\
\mathcal{W}^{(2)} &= \lambda_1^{(2)}(x^2 - y^2) \\
\mathcal{W}^{(3)} &= \lambda_1^{(3)}(x^3 + xy^2) \\
\mathcal{W}^{(4)} &= \lambda_1^{(4)}(x^4 - y^4) + \lambda_2^{(4)}(x^4 - 6x^2y^2 + y^4) \\
\mathcal{W}^{(5)} &= \lambda_1^{(5)}(x^5 + 2x^3y^2 + xy^4) + \lambda_2^{(5)}(x^5 - 4x^3y^2 + 3xy^4) \\
\mathcal{W}^{(6)} &= \lambda_1^{(6)}(x^6 + x^4y^2 - x^2y^4 - y^6) + \lambda_2^{(6)}(x^6 - 5x^4y^2 - 5x^2y^4 + y^6)
\end{aligned} \tag{11}$$

$$\begin{aligned}
\mathcal{Z}^{(1)} &= \lambda_1^{(1)}y \\
\mathcal{Z}^{(2)} &= \lambda_1^{(2)}(-2xy) \\
\mathcal{Z}^{(3)} &= \lambda_1^{(3)}(x^2y + y^3) \\
\mathcal{Z}^{(4)} &= \lambda_1^{(4)}(-2x^3y - 2xy^3) + \lambda_2^{(4)}(4x^3y - 4xy^3) \\
\mathcal{Z}^{(5)} &= \lambda_1^{(5)}(x^4y + 2x^2y^3 + y^5) + \lambda_2^{(5)}(-2x^4y + 6x^2y^3) \\
\mathcal{Z}^{(6)} &= \lambda_1^{(6)}(-2x^5y - 4x^3y^3 - 2xy^5) + \lambda_2^{(6)}(4x^5y - 4xy^5)
\end{aligned} \tag{12}$$

where $\mathcal{V}^{(n)}$ is the nth order of the trace and $\mathcal{W}^{(n)}$ and $\mathcal{Z}^{(n)}$ are the nth order diagonal and off-diagonal elements, respectively, of the traceless JT Hamiltonian. The polynomial expansions presented here differ, at the first look, from those of Viel and Eisfeld [17]. However, they are interconvertable by taking linear combinations. As an illustration, the number of free parameters to be optimized for an 8th order expansion is given in tabular form in Table 1. Note that the number of independent optimization parameters grows very slowly with the order of the expansion, which reflects the high inherent symmetry of the $E \times e$ JT Hamiltonian.

Table 1. Number of parameters in the trace and the diagonal and off-diagonal terms in the $E \times e$ JT expansion in each order.

order	1	2	3	4	5	6	7	8
parameters $\mathcal{W}, \mathcal{Z}$	1	1	1	2	2	2	3	3
parameters $\mathcal{V}$	0	1	1	1	1	2	1	2
total	1	2	2	3	3	4	4	5

As an example, the sixth order $E \times e$ JT Hamiltonian matrix is given explicitly in Eq. (13). It can be seen that the sixth-order JT Hamiltonian contains only 4 independent optimization parameters.

$$\mathcal{H}^{(6)} = [a_1^{(6)}(x^6 + 3x^4y^2 + 3x^2y^4 + y^6) + a_2^{(6)}(x^6 - 6x^4y^2 + 9x^2y^4)]\ \mathbf{1}$$

$$+ \begin{pmatrix} \lambda_1^{(6)}(x^6 + x^4y^2 - x^2y^4 - y^6) & \lambda_1^{(6)}(-2x^5y - 4x^3y^3 - 2xy^5) \\ +\lambda_2^{(6)}(x^6 - 5x^4y^2 - 5x^2y^4 + y^6) & +\lambda_2^{(6)}(4x^5y - 4xy^5) \\ \\ \lambda_1^{(6)}(-2x^5y - 4x^3y^3 - 2xy^5) & -\lambda_1^{(6)}(x^6 + x^4y^2 - x^2y^4 - y^6) \\ +\lambda_2^{(6)}(4x^5y - 4xy^5) & -\lambda_2^{(6)}(x^6 - 5x^4y^2 - 5x^2y^4 + y^6) \end{pmatrix}. \tag{13}$$

Using Weyl's polarization method [41], it is straightforward to include an arbitrary number of e modes to obtain the $E \times (e + e + \cdots)$ JT Hamiltonian up to arbitrary order.

2.3. The $T_2 \times t_2$ Jahn-Teller Hamiltonian

The three-sheeted $T_2 \times t_2$ PE surface is represented by three diabatic electronic states of T_2 symmetry, denoted conveniently as x, y, z. The nuclear coordinates of t_2 symmetry are also denoted by x, y, z to reveal the high inherent symmetry of the $T_2 \times t_2$ JT Hamiltonian. The ring of invariant polynomials of the t_2 representation in T_d is finitely generated by a set of three polynomials of degree 2, 3 and 4 in the coordinates x, y, z [23, 42]

$$\begin{aligned} f_1 &= x^2 + y^2 + z^2 \\ f_2 &= xyz \\ f_3 &= x^4 + y^4 + z^4. \end{aligned} \tag{14}$$

Any member of the ring $\mathbb{K}[x, y, z]^{T_d}$ can be represented in terms of these generating polynomials, that is

$$\mathbb{K}[x, y, z]^{T_d} = \mathbb{K}[f_1, f_2, f_3]. \tag{15}$$

The JT vibronic matrix is given by the doubly polarized invariant polynomials in the combined vector spaces of the electronic coefficients and the nuclear coordinates, which transform identically under the group $T_d \simeq S_4$. Any term of the Hamiltonian matrix expansion is just the Hessian of an invariant polynomial of the ring $\mathbb{K}[x, y, z]^{T_d}$ up to multiplication with a constant factor.

An elegant combinatorial scheme has been developed to represent the $T_2 \times t_2$ JT PE matrix in terms of the generating polynomials in Ref. [23]. The JT vibronic matrix has the highly

symmetric structure

$$\mathcal{H}_{el} = \begin{pmatrix} \mathcal{W}(x,y,z) & \mathcal{Z}(z,x,y) & \mathcal{Z}(y,x,z) \\ \mathcal{Z}(z,x,y) & \mathcal{W}(y,x,z) & \mathcal{Z}(x,y,z) \\ \mathcal{Z}(y,x,z) & \mathcal{Z}(x,y,z) & \mathcal{W}(z,x,y) \end{pmatrix}. \tag{16}$$

Where $\mathcal{W}$ and $\mathcal{Z}$ are the diagonal and off-diagonal elements of the JT matrix, respectively. Their expansion up to sixth order reads

$$\begin{aligned}
\mathcal{W}^{(1)}(x,y,z) &= 0 \\
\mathcal{W}^{(2)}(x,y,z) &= a_1^{(2)}x^2 + a_2^{(2)}(y^2+z^2) \\
\mathcal{W}^{(3)}(x,y,z) &= a_1^{(3)}xyz \\
\mathcal{W}^{(4)}(x,y,z) &= a_1^{(4)}x^4 + a_2^{(4)}(y^4+z^4) \\
&\quad + a_3^{(4)}(x^2y^2+x^2z^2+y^2z^2) \\
\mathcal{W}^{(5)}(x,y,z) &= a_1^{(5)}x^3yz + a_2^{(5)}(xy^3z+xyz^3) \\
\mathcal{W}^{(6)}(x,y,z) &= a_1^{(6)}(y^6+z^6) + a_2^{(6)}x^6 + a_3^{(6)}(x^4y^2+x^4z^2) \\
&\quad + a_4^{(6)}(x^2y^4+x^2z^4) + a_5^{(6)}(y^4z^2+y^2z^4) + a_6^{(6)}x^2y^2z^2 \\
\mathcal{Z}^{(1)}(x,y,z) &= b_1^{(1)}x \\
\mathcal{Z}^{(2)}(x,y,z) &= b_1^{(2)}yz \\
\mathcal{Z}^{(3)}(x,y,z) &= b_1^{(3)}x^3 + b_2^{(3)}(xy^2+xz^2) \\
\mathcal{Z}^{(4)}(x,y,z) &= b_1^{(4)}x^2yz + b_2^{(4)}(y^3z+yz^3) \\
\mathcal{Z}^{(5)}(x,y,z) &= b_1^{(5)}x^5 + b_2^{(5)}(x^3y^2+x^3z^2) \\
&\quad + b_3^{(5)}(xy^4+xz^4) + b_4^{(5)}(xy^2z^2) \\
\mathcal{Z}^{(6)}(x,y,z) &= b_1^{(6)}y^3z^3 + b_2^{(6)}(y^4z^2+y^2z^4) \\
&\quad + b_3^{(6)}x^4yz + b_4^{(6)}(x^2y^3z+x^2yz^3).
\end{aligned} \tag{17}$$

The expansion terms up to 12th order can be found in Ref. [23]. The beauty of this representation is that the elements of the 3×3 JT matrix consist of just two functions, whose position in the matrix is determined by the first argument. There are only two kinds of parameters, $a_i^{(n)}$ and $b_i^{(n)}$ which are to be determined by a least-squares fitting of *ab initio* data. The number of parameters to be optimized for an 8th-order expansion of the $T_2 \times t_2$ PE matrix is summarized in Table 2.

Table 2. Number of parameters in the diagonal and off-diagonal terms in the $T_2 \times t_2$ JT matrix in each order.

order	1	2	3	4	5	6	7	8
parameters $\mathcal{W}$	0	2	1	3	2	6	4	9
parameters $\mathcal{Z}$	1	1	2	2	4	4	6	6
total	1	3	3	5	6	10	10	15

The 8th order PE matrix, for example, contains 53 parameters.

It is straightforward to include an arbitrary number of t_2 modes in this approach. Weyl's polarization method provides a convenient scheme to obtain the generators for several t_2 coordinates. There are 12 generators in total for the $T_2 \times (t_2 + t_2)$ matrix expansion, for example [23].

2.4. Application : The E×e Jahn-Teller effect in P_4^+

P_4^+ is a system exhibiting an extremely strong JT effect in its electronic ground state of ^2E symmetry involving the doubly degenerate (e) bending mode. The $^2E \times e$ JT effect in P_4^+ with a dimensionless linear JT coupling parameter of about 5.0 [43, 57] may be the strongest $E \times e$ JT effect known in nature. The first *ab initio* investigation of the JT effect in the ^2E state of P_4^+ was carried out by Meiswinkel and Köppel [43] in the early 1990s. A more recent investigation was performed by Opalka et al.

The *ab initio* PE data were calculated at the CASSCF/cc-pVDZ level of theory using the MOLPRO quantum chemistry package [44]. The parameters of the polynomial expansion have been obtained by fitting the eigenvalues of the PE matrix to the *ab initio* data. *Ab initio* energies up to 2 eV above the energy at the reference geometry (the equilibrium geometry of P_4) have been calculated. A total of 1100 energy points have been included in the least-squares fitting. The difference between a fit including terms up to second order and a fit including terms up to sixth order is illustrated in Fig. 1. The figure confirms the necessity to extend the JT expansion beyond the standard model in this system. For the second-order fit, the *ab initio* data in the range $-0.35 \leq s_{2y} \leq 0.35$ (in Å) have been included. For the 6th-order fit, the *ab initio* data in the range $-0.8 \leq s_{2y} \leq 0.8$ (in Å) have been taken into account. Fig. (1) clearly shows that the second-order approximation is insufficient for an accurate representation of the *ab initio* PE surface of the ^2E ground state of P_4^+. Due to intra-molecular collisions which occur at large displacements from the equilibrium geometry in the e modes, the $E \times e$ JT PE surface exhibits a strong positive anharmonicity. An rms residual error of 0.02 eV has been estimated for the 6th-order surface for energies below 2.0 eV.

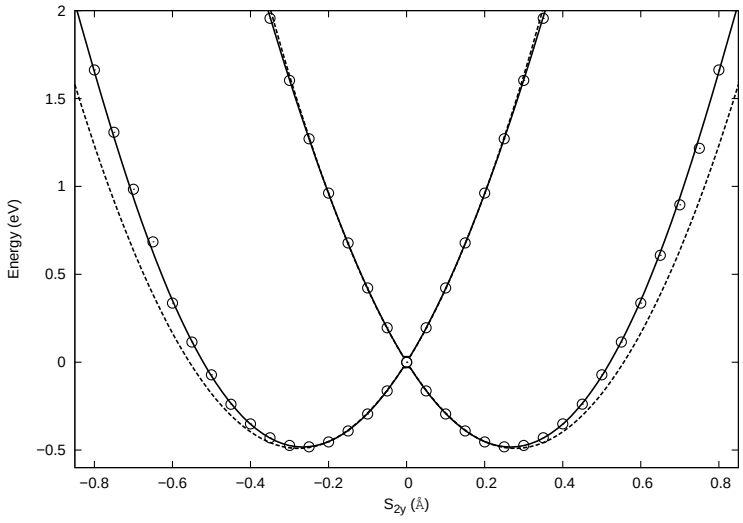

Figure 1. Cut of the 2nd order (dashed line) and the 6th order (full line) PE surface of the electronic ground state of P_4^+ along the symmetry coordinate s_{2y} compared with the *ab initio* data (circles).

The importance of JT coupling terms up to 6th order for an accurate representation of $E \times e$ JT PE surfaces has also been demonstrated for NH_3^+ [20], NO_3 [19] and various transition metal trifluorides of D_{3h} symmetry [21, 22].

The experimental photoelectron spectra of P_4, As_4 and Sb_4 were reported by several groups more than 20 years ago [53–56]. It was found that these cluster cations exhibit very strong JT effects, involving the e mode in the ^2E ground state and the t_2 mode in the $^2T_2$ excited state. In addition, the effects of (zeroth-order) SO splitting were identified in the JT spectra of As_4^+ and Sb_4^+ [53–56].

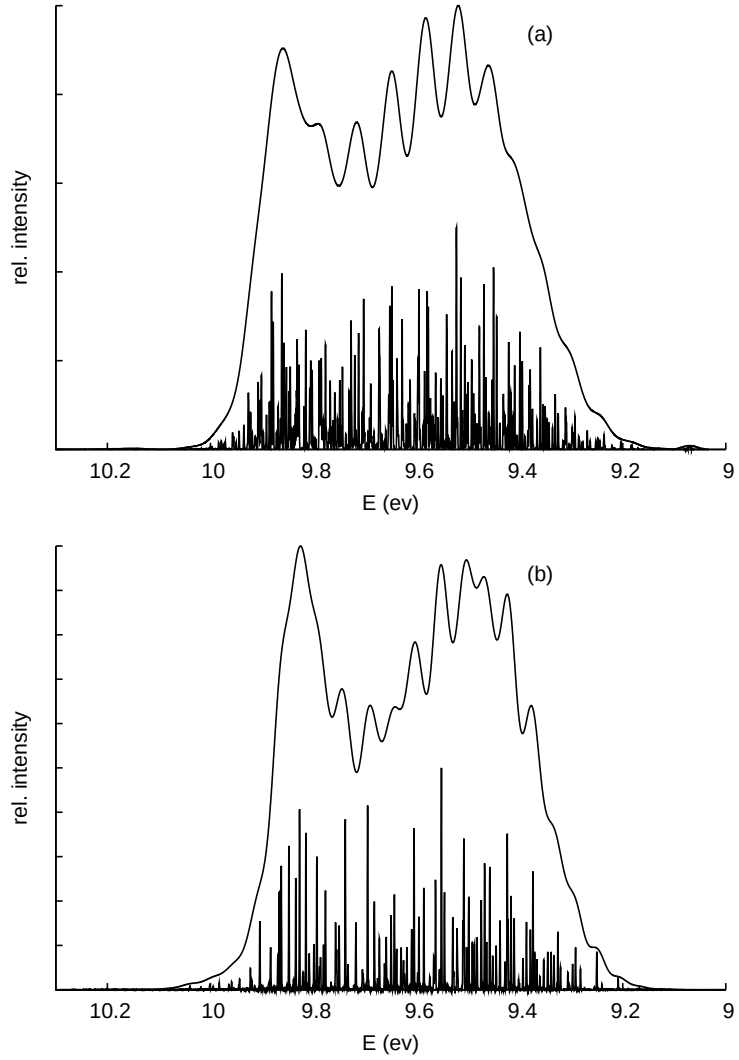

Figure 2. $^2E \times e$ JT spectrum of P_4^+ obtained with the quadratic (a) and the 6th-order (b) JT Hamiltonian

The photoelectron spectrum of the ^2E state of P_4^+ was calculated via the time-dependent approach to molecular electronic spectra [59, 60] as the Fourier transform of the autocorrelation function [58]. The propagation of the wave packet on the coupled diabatic PE surfaces was performed with the Chebysheff method [61] (see Ref. [58] for details). The so-called "low-resolution spectrum" is obtained by convolution with a Gaussian of 35 meV full width at half maximum. To obtain a "high-resolution spectrum" the full width at half maximum has been reduced by a factor of 1/30. The ^2E photoelectron spectrum of P_4^+ including up to quadratic JT coupling is shown in Fig. 2a. The clear double-hump structure of the envelope is due to a very

strong linear JT coupling. The high line density and irregular structure of the high-resolution spectrum arise from quadratic JT coupling. Fig. 2b shows the photoelectron spectrum calculated with the inclusion of JT coupling terms up to 6th order. While the low-resolution envelopes of the two spectra are similar, the line density is reduced in the 6th-order spectrum as a result of the significant positive anharmonocity of the potential.

3. Expansion of the spin-orbit coupling Hamiltonian beyond zeroth order

3.1. Relativistically generalized Jahn-Teller selection rules

The symmetry group of the Hamiltonian including electron spin and SO coupling is the so-called spin double group of the respective point group [45]. The elements of the spin double group are of the form

$$Z_n = C_n U_n^\dagger \tag{18}$$

where the C_n are the symmetry operators of the point group and the U_n are unitary 2×2 matrices acting on the two-component spinors (or the spin functions α, β in the nonrelativistic limit). To close the group, the operator $-Z_n$ has to be included for every Z_n of Eq. (18), which doubles the order of the group [45]. The character tables of the common spin double groups can be found, for example, in Ref. [46].

Consider the group C_{3v} as one of the simplest non-Abelian point groups. The spin-free JT selection rule in the C_{3v} point group is [1]

$$[E^2] = A + E \tag{19}$$

where $[\Gamma^2]$ denotes the symmetrized square of the irreducible representation Γ [45]. According to Eq. (19), vibrational modes of e symmetry are JT active in first order. The relativistically generalized selection rules in the spin double group C'_{3v} are (for a single unpaired electron)

$$^2E = E \times E_{1/2} = E_{1/2} + E_{3/2} \tag{20a}$$

$$E_{1/2} \times E_{3/2} = 2E \tag{20b}$$

where $E_{1/2}$ and $E_{3/2}$ are two-dimensional two-valued irreducible representations of C'_{3v}. The spin function of a single electron transforms as $E_{1/2}$ in C'_{3v}. According to Eq. (20a), the four-fold degenerate ^2E state splits into two-fold degenerate $E_{1/2}$ and $E_{3/2}$ states by SO coupling. According to Eq. (20b), vibrational modes of e symmetry can couple the $E_{1/2}$ and $E_{3/2}$ SO-split electronic states. Since the e modes are already JT active in the electrostatic Hamiltonian, no new JT couplings arise from the SO operator. This has been confirmed by the explicit construction of the $^2E \times e$ JT Hamiltonian with inclusion of SO coupling [26]. In C_{3v} systems, the SO operator thus lifts the degeneracy of the nonrelativistic ^2E state, while the JT forces are of electrostatic origin [47].

Interestingly, a different situation is encountered in the tetragonal groups (D_{2d}, C_{4v}, D_{4h}). In the D_{2d} group, the spin-free selection rule is

$$[E^2] = A_1 + B_1 + B_2. \tag{21}$$

As is well known, the nondegenerate b_1 and b_2 normal modes are JT active (in first order) in tetragonal systems [4–6, 10]. The relativistically generalized selection rules in the D'_{2d} spin double group are

$$^2E = E \times E_{1/2} = E_{1/2} + E_{3/2} \tag{22a}$$

$$E_{1/2} \times E_{3/2} = B_1 + B_2 + E. \tag{22b}$$

According to Eq. (22a), the SO interaction lifts the four-fold degeneracy of the ^2E state. According to Eq. (22b), the $E_{1/2}$ and $E_{3/2}$ components of the SO-split ^2E state are coupled in first order by b_1, b_2 and e modes. Since the e modes are not JT active at the electrostatic level (see Eq. (21)), the JT activity of the e modes must arise from the SO operator. The same selection rules apply in C'_{4v} and D'_{4h}. The relativistic JT forces are thus complementary to the electrostatic JT forces in tetragonal systems.

In tetrahedral systems (point group T_d), the spin-free selection rules are [4–7, 10]

$$[E^2] = A_1 + E \tag{23a}$$

$$[T_{1,2}^2] = A_1 + E + T_2. \tag{23b}$$

The vibrational modes transform as a_1, e or t_2 in T_d. In electronic states of E symmetry, only the modes of e symmetry are JT active in first order (Eq. (23a)). In electronic states of T_1 or T_2 symmetry, the t_2 modes as well as the e modes are JT active (Eq. (23b)). $^2T_1$, $^2T_2$ and ^2E electronic states transform as follows in T'_d:

$$^2T_1 = T_1 \times E_{1/2} = G_{3/2} + E_{1/2} \tag{24a}$$

$$^2T_2 = T_2 \times E_{1/2} = G_{3/2} + E_{5/2} \tag{24b}$$

$$^2E = E \times E_{1/2} = G_{3/2} \tag{24c}$$

where $E_{1/2}$, $E_{5/2}$ are two-dimensional double-valued irreducible representations, while $G_{3/2}$ is a four-dimensional double-valued irreducible representation of T'_d [48]. According to Eqs. (24a, 24b), $^2T_1$ ($^2T_2$) electronic states split into $G_{3/2}$ and $E_{1/2}$ ($E_{5/2}$) irreducible components by SO coupling. The four-fold degeneracy of a ^2E electronic state, on the other hand, is not lifted by SO coupling at the tetrahedral reference geometry (Eq. 24c). While the two-fold degeneracy of the $E_{1/2}$ and $E_{5/2}$ levels cannot be lifted by any intramolecular interaction (Kramers degeneracy [49]), the energy levels of $G_{3/2}$ can split into two two-fold degenerate levels.

The JT selection rules in the T'_d spin double group are

$$E_{1/2} \times G_{3/2} = E + T_1 + T_2 \tag{25a}$$

$$E_{5/2} \times G_{3/2} = E + T_1 + T_2 \tag{25b}$$

$$\left\{G_{3/2}^2\right\} = A_1 + E + T_2. \tag{25c}$$

Here $\{\Gamma^2\}$ denotes the antisymmetrized product of Γ [45, 50]. Eq. (25c) reveals that the degeneracy of a $G_{3/2}$ electronic state is unstable with respect to deformations via e and t_2 modes. For a ^2E state, which transforms as $G_{3/2}$ in T'_d (Eq. (24c)), the t_2 mode is not JT active at the electrostatic level, see Eq. (23a). It follows that the JT activity of the t_2 modes in ^2E states must arise form the SO operator. A more detailed analysis (see below) reveals that in $^2T_{1,2}$ states the t_2 modes and the e modes are JT active (in first order) via electrostatic as well as relativistic forces. In ^2E states, on the other hand, the JT activity of the e modes is of electrostatic origin, while the JT activity of the t_2 modes is of relativistic origin [27, 28]. The JT selection rules in cubic symmetry (O_h, O'_h) are the same as in Eq. (23-25), apart from the additional inversion symmetry.

The relativistically generalized selection rules for electronic states of higher spin multiplicity in odd-electron systems can be obtained by a straightforward extension of the above analysis, since the representation of quartet, sextet, etc. spin states can be decomposed into the two-valued irreducible representations of the spin double group. In even-electron systems, the electronic states transform according to single-valued irreducible representations of the spin double group.

3.2. Relativistic $^2E \times e$ Jahn-Teller effect in D_{2d} systems

Let us consider, as the simplest model of a D_{2d}-symmetric object, a covalently bonded five-atomic YX_4 system, where Y is the central atom and the YX_1X_2 and YX_3X_4 atoms are in planes which are oriented perpendicular to each other. Aluminium tetroxide (AlO_4) is an example.

For the purpose of symmetry analysis, the electrostatic Hamiltonian is written as (in atomic units)

$$\mathcal{H}_{es} = -\frac{1}{2}\nabla^2 - \Phi(\mathbf{r}) \tag{26a}$$

$$\Phi(\mathbf{r}) = \frac{Q_0}{r} + \sum_{k=1}^{4} \frac{Q_1}{r_k} \tag{26b}$$

where Q_0 and Q_1 are effective atomic charges, $\mathbf{r}$ is the radius vector of the electron, $r = |\mathbf{r}|$ and $r_k = |\mathbf{r} - \mathbf{R}_k|$. The $\mathbf{R}_k$, $k = 1 \ldots 4$, are the radius vectors to the atoms $X_1 \ldots X_4$. The Y atom is at the origin of the coordinate system.

The Breit-Pauli operator for this system reads [31]

$$\mathcal{H}_{SO} = -ig_e\beta_e^2\mathbf{S}\left[\frac{Q_0}{r^3}(\mathbf{r}\times\boldsymbol{\nabla}) + Q_1\sum_{k=1}^{4}\frac{1}{r_k^3}(\mathbf{r}_k\times\boldsymbol{\nabla})\right] \tag{27a}$$

where

$$\mathbf{S} = \frac{1}{2}(\mathbf{i}\sigma_x + \mathbf{j}\sigma_y + \mathbf{k}\sigma_z), \tag{27b}$$

σ_x, σ_y, σ_z are the Pauli spin matrices, β_e is the Bohr magneton, g_e is the g-factor of the electron, and $\mathbf{i}$, $\mathbf{j}$, $\mathbf{k}$ are the Cartesian unit vectors.

We consider an isolated electronic E orbital with diabatic wave functions ψ_x, ψ_y which transform as x, y in the D_{2d} point group. The four-dimensional Hilbert space of a single electron in the E orbital is spanned by the spin-orbital basis functions

$$\{\psi_x\alpha, \psi_y\alpha, \psi_y\beta, \psi_x\beta\}\,. \tag{28}$$

The nine vibrational coordinates of the YX_4 molecule transform as

$$\Gamma_v = 2a_1 + b_1 + 2b_2 + 2e \tag{29}$$

in the D_{2d} point group. According to the selection rules of Eqs. (21,22), the b_1, b_2 and e modes are JT active in first order. In the following we consider, for brevity and clarity, only one representative of the b_1, b_2 and e modes, respectively. We denote the nondegenerate normal coordinates of b_1, b_2 symmetry as q_1, q_2, and the normal coordinates of e symmetry as q_x, q_y.

The spin-free Hamiltonian $\mathcal{H}_{es}$ is expanded, as usual, up to second order in normal coordinates of b_1, b_2 and e symmetry (see Ref. [30] for details). The Breit-Pauli operator is expanded up to first order in the normal modes. This expansion can be written as

$$\mathcal{H}_{SO} = \mathcal{H}_{SO}^{(0)} + \mathcal{H}_{SO}^{(1)} \tag{30a}$$

$$\mathcal{H}_{SO}^{(0)} = [h^y(e)\sigma_y + h^x(e)\sigma_x] + h^z(a_2)\sigma_z \tag{30b}$$

$$\begin{aligned}\mathcal{H}_{SO}^{(1)} =& [h_1^x(e)q_1\sigma_x + h_1^y(e)q_1\sigma_y] + [h_2^y(e)q_2\sigma_y - h_2^x(e)q_2\sigma_x] \\ &+ [h_y^z(e)q_y\sigma_z - h_x^z(e)q_x\sigma_z] + h_1^z(b_2)q_1\sigma_z + h_2^z(b_1)q_2\sigma_z \\ &+ h_+(b_1)(q_x\sigma_x + q_y\sigma_y) + h_-(a_2)(q_x\sigma_x - q_y\sigma_y) \\ &+ h^+(a_1)(q_x\sigma_y + q_y\sigma_x) + h^-(b_2)(q_x\sigma_y - q_y\sigma_x).\end{aligned} \tag{30c}$$

The expansion coefficients in Eqs. (30b, 30c) are operators in electronic coordinate space. Their transformation properties are indicated in parentheses. The square brackets indicate symmetry-adapted linear combinations.

The ${}^2E \times (b_1 + b_2 + e)$ SO Hamiltonian matrix is obtained by calculating the matrix elements of $\mathcal{H}_{SO}$ with the electronic basis functions (28). The result is [30]

$$\mathcal{H}_{SO}[{}^2E \times e] = \begin{pmatrix} 0 & i\Delta & i\gamma q_+ & 0 \\ -i\Delta & 0 & 0 & -i\gamma q_+ \\ -i\gamma q_- & 0 & 0 & i\Delta \\ 0 & i\gamma q_- & -i\Delta & 0 \end{pmatrix} \tag{31a}$$

where

$$q_\pm = q_x \pm i q_y. \tag{31b}$$

Here Δ is the zeroth-order SO coupling which gives rise to the SO splitting of the ${}^2E$ state at the reference geometry. The real parameter γ represents the linear JT coupling arising from the SO operator. In the real-valued spin-orbital basis (28) the diagonal elements of the Breit-Pauli operator are necessarily zero, since the latter is purely imaginary (see Eq. (27a)). However, at the reference geometry ($q_x = q_y = 0$) the Hamiltonian matrix can be diagonalized, yielding the eigenvalues $-\Delta$, $-\Delta$, Δ, Δ. Due to the Kramers degeneracy of the eigenvalues, the unitary transformation is not unique. A suitable choice is [30]

$$U = \frac{1}{\sqrt{2}} \begin{pmatrix} 1 & 1 & 0 & 0 \\ -i & i & 0 & 0 \\ 0 & 0 & 1 & 1 \\ 0 & 0 & -i & i \end{pmatrix}. \tag{32}$$

This transformation defines a SO-adapted diabatic electronic basis.

Including the electrostatic JT coupling terms up to first order, the linear ${}^2E \times (b_1 + b_2 + e)$ JT coupling matrix in the SO-adapted basis reads

$$\widetilde{\mathcal{H}}^{(1)}[{}^2E \times (b_1 + b_2 + e)] = E_E \mathbf{1}_4 + \begin{pmatrix} \Delta & bq_2 + iaq_1 & 0 & i\gamma q_+ \\ bq_2 - iaq_1 & -\Delta & i\gamma q_+ & 0 \\ 0 & -i\gamma q_- & \Delta & -bq_2 + iaq_1 \\ -i\gamma q_- & 0 & -bq_2 - iaq_1 & -\Delta \end{pmatrix}. \tag{33}$$

Here $\mathbf{1}_4$ denotes the 4×4 unit matrix and a, b are the linear JT coupling constants of the b_1, b_2 modes. When the electrostatic JT couplings are neglected ($a = b = 0$), the Hamiltonian matrix (37) becomes isomorphic with the linear ${}^2E \times e$ JT+SO coupling Hamiltonian of trigonal systems [47].

The vibronic matrix (33) can easily be diagonalized, since the quartic secular polynomial factorizes into two quadratic polynomials due to time-reversal symmetry. The eigenvalues are given by

$$V_1 = V_2 = E_E - \sqrt{\Delta^2 + a^2 q_1^2 + b^2 q_2^2 + \gamma^2 (q_x^2 + q_y^2)} \tag{34a}$$

$$V_3 = V_4 = E_E + \sqrt{\Delta^2 + a^2 q_1^2 + b^2 q_2^2 + \gamma^2 (q_x^2 + q_y^2)}. \tag{34b}$$

They represent five-dimensional elliptic hyperboloids (the energies as a function of four nuclear coordinates). The Hamiltonian matrix and adiabatic potentials with inclusion of the quadratic electrostatic expansion terms can be found in Ref. [30].

Although the D_{2d} group is one of the less common point groups, it certainly is of relevance for the theoretical description of photochemical reactions. The D_{2d} group, being a subgroup of the tetrahedral and cubic groups, is a frequently occurring epikernel group in tetrahedral and cubic systems, that is, it is associated with local minima of the multi-dimensional JT PE surfaces [51]. The determination of JT and SO couplings at stationary points of D_{2d} symmetry is thus of widespread relevance in the theoretical analysis of transition-metal complexes, organometallic compounds and crystals.

3.3. Relativistic ${}^2T_2 \times t_2$ and ${}^2E \times t_2$ Jahn-Teller effect in tetrahedral and octahedral systems
Let us consider a four-atomic tetrahedral system with a single unpaired electron. Examples are the cluster cations P_4^+, As_4^+, Sb_4^+, Bi_4^+. The point group of the electrostatic Hamiltonian is T_d; the point group of the SO operator is T_d'. For the purpose of symmetry analysis, the electrostatic Hamiltonian of the unpaired electron is approximated as

$$\mathcal{H}_{es} = -\frac{1}{2}\nabla^2 - \Phi(\mathbf{r}) \tag{35a}$$

$$\Phi(\mathbf{r}) = Q\sum_{k=1}^{4}\frac{1}{r_k} \tag{35b}$$

where Q is the effective nuclear charge of the four equivalent atoms. The r_k are defined analogously to Eq. (26).

The Breit-Pauli operator for this system reads [31]

$$\mathcal{H}_{SO} = -ig_e\beta_e^2 Q\mathbf{S}\sum_{k=1}^{4}\frac{1}{r_k^3}(\mathbf{r}_k \times \boldsymbol{\nabla}) \tag{36}$$

where $\mathbf{S}$ is defined in Eq. (27b).

Molecular orbitals transforming according to the T_2 representation can be constructed as linear combinations of atomic p orbitals $\varphi_x^{(k)}$, $\varphi_y^{(k)}$, $\varphi_z^{(k)}$ on the four atoms

$$\psi_j = \frac{1}{2}\sum_{k=1}^{4}\varphi_j^{(k)}, \qquad j = x, y, z. \tag{37}$$

The six-dimensional Hilbert space of a single electron in the T_2 orbital is spanned by the spin-orbital basis functions

$$\{\psi_x\alpha, \psi_y\alpha, \psi_z\alpha, \psi_z\beta, \psi_y\beta, \psi_x\beta\}\,. \tag{38}$$

The six vibrational coordinates of the X_4 system transform as

$$\Gamma_v = a_1 + t_2 + e \tag{39}$$

in the T_d point group. According to the selection rule (23b), the t_2 and e modes are JT active in first order. We consider only the normal modes of t_2 symmetry in what follows and denote the normal coordinates of t_2 symmetry as Q_x, Q_y, Q_z.

The spin-free Hamiltonian $\mathcal{H}_{es}$ is expanded, as usual, up to second order in the normal coordinates of t_2 symmetry. The Breit-Pauli operator is expanded up to first order

$$\mathcal{H}_{SO} = \mathcal{H}_{SO}^{(0)} + \mathcal{H}_{SO}^{(1)} \tag{40a}$$

$$\mathcal{H}_{SO}^{(0)} = h^x\sigma_x + h^y\sigma_y + h^z\sigma_z \tag{40b}$$

$$\begin{aligned}\mathcal{H}_{SO}^{(1)} =& h(a_2)P_{a_2} + h(e_a)P_{e_a} + h(e_b)P_{e_b} \\ &+ h(t_{1x})P_{t_{1x}} + h(t_{1y})P_{t_{1y}} + h(t_{1z})P_{t_{1z}} \\ &+ h(t_{2x})P_{t_{2x}} + h(t_{2y})P_{t_{2y}} + h(t_{2z})P_{t_{2z}}\end{aligned} \tag{40c}$$

where the P_j are first-order symmetry adapted polynomials in $\mathbf{Q}$, defined as

$$P_{a_2}(\mathbf{Q},\boldsymbol{\sigma}) = \frac{1}{\sqrt{3}}(Q_x\sigma_x + Q_y\sigma_y + Q_z\sigma_z) \tag{41a}$$

$$P_{e_a}(\mathbf{Q},\boldsymbol{\sigma}) = \frac{1}{\sqrt{6}}(2Q_x\sigma_x - Q_y\sigma_y - Q_z\sigma_z) \tag{41b}$$

$$P_{e_b}(\mathbf{Q},\boldsymbol{\sigma}) = \frac{1}{\sqrt{2}}(Q_y\sigma_y - Q_z\sigma_z) \tag{41c}$$

$$P_{t_{1x}}(\mathbf{Q},\boldsymbol{\sigma}) = \frac{1}{\sqrt{2}}(Q_z\sigma_y - Q_y\sigma_z) \tag{41d}$$

$$P_{t_{2x}}(\mathbf{Q},\boldsymbol{\sigma}) = \frac{1}{\sqrt{2}}(Q_z\sigma_y - Q_y\sigma_z). \tag{41e}$$

The $P_{t_{1y}}$, $P_{t_{1z}}$ and $P_{t_{2y}}$, $P_{t_{2z}}$ follow by cyclic permutation.

The ${}^2T_2 \times t_2$ SO Hamiltonian matrix is obtained by calculating the matrix elements of $\mathcal{H}_{SO}$ with the electronic basis functions (38). The result is [28]

$$\mathcal{H}^{(0)}_{SO}[T_2] = \Delta \begin{pmatrix} 0 & i & 0 & -1 & 0 & 0 \\ -i & 0 & 0 & i & 0 & 0 \\ 0 & 0 & 0 & 0 & -i & 1 \\ -1 & -i & 0 & 0 & 0 & 0 \\ 0 & 0 & i & 0 & 0 & i \\ 0 & 0 & 1 & 0 & -i & 0 \end{pmatrix} \tag{42}$$

$$\mathcal{H}^{(1)}_{SO}[T_2 \times t_2] = \alpha \begin{pmatrix} 0 & 0 & -iQ_x & -iQ_z & Q_+ & 0 \\ 0 & 0 & iQ_y & Q_z & 0 & -Q_+ \\ iQ_x & -iQ_y & 0 & 0 & -Q_z & iQ_z \\ iQ_z & Q_z & 0 & 0 & iQ_y & -iQ_x \\ Q_- & 0 & -Q_z & -iQ_y & 0 & 0 \\ 0 & -Q_- & -iQ_z & iQ_x & 0 & 0 \end{pmatrix} \tag{43}$$

where

$$Q_\pm = Q_x \pm iQ_y. \tag{44}$$

Here Δ is the zeroth-order SO splitting of the ${}^2T_2$ state and α is the linear relativistic ${}^2T_2 \times t_2$ JT coupling constant.

The Hermitian matrix $\mathcal{H}^{(0)}_{SO}$ of Eq. (42) can be diagonalized by a unitary transformation U. Since the transformed matrix $\widetilde{\mathcal{H}}^{(0)}_{SO}$ has degenerate eigenvalues, the unitary matrix U is not unique. A suitable choice is given in Appendix B of Ref. [28] and defines a SO-adapted electronic basis. The zeroth-order SO vibronic matrix takes the form

$$\mathcal{H}^{(0)}_{SO}[T_2] = \mathrm{diag}(-\Delta, -\Delta, -\Delta, -\Delta, 2\Delta, 2\Delta). \tag{45}$$

In agreement with the group-theoretical result (24b), the zeroth-order SO coupling splits the six-fold degenerate ${}^2T_2$ manifold into a quadruply degenerate manifold ($G_{3/2}$) and a doubly degenerate manifold ($E_{5/2}$) [48].

Including the electrostatic JT coupling terms up to first order, the linear ${}^2T_2 \times t_2$ JT coupling

Hamiltonian in the SO adapted basis reads [28]

$$\widetilde{\mathcal{H}}^{(1)}[^2T_2 \times t_2] = E_{T_2}\mathbf{1}_6 + \begin{pmatrix} -\Delta & -i\tilde{a}_1Q_+ & 0 & i\tilde{a}_1Q_z & 0 & i\tilde{a}_2Q_- \\ i\tilde{a}_1Q_- & -\Delta & -i\tilde{a}_1Q_z & 0 & -\frac{i}{\sqrt{3}}\tilde{a}_2Q_- & \frac{2i}{\sqrt{3}}\tilde{a}_2Q_z \\ 0 & i\tilde{a}_1Q_z & -\Delta & i\tilde{a}_1Q_- & -i\tilde{a}_2Q_+ & 0 \\ -i\tilde{a}_1Q_z & 0 & -i\tilde{a}_1Q_+ & -\Delta & -\frac{2i}{\sqrt{3}}\tilde{a}_2Q_z & -\frac{i}{\sqrt{3}}\tilde{a}_2Q_+ \\ 0 & \frac{i}{\sqrt{3}}\tilde{a}_2Q_+ & i\tilde{a}_2Q_- & \frac{2i}{\sqrt{3}}\tilde{a}_2Q_z & 2\Delta & 0 \\ -i\tilde{a}_2Q_+ & -\frac{2i}{\sqrt{3}}\tilde{a}_2Q_z & 0 & \frac{i}{\sqrt{3}}\tilde{a}_2Q_- & 0 & 2\Delta \end{pmatrix} \tag{46a}$$

where

$$\tilde{a}_1 = \frac{1}{\sqrt{3}}(a + 2\alpha) \tag{46b}$$

$$\tilde{a}_2 = \frac{1}{\sqrt{2}}(a - \alpha) \tag{46c}$$

and a is the linear electrostatic $T_2 \times t_2$ JT coupling constant. It is seen that the effective linear JT coupling parameters in the SO-adapted basis have an electrostatic (a) and relativistic (α) contribution. The parameter $\tilde{a}_1$ is the effective linear JT coupling constant of the $G_{3/2}$ manifold. The parameter $\tilde{a}_2$ describes the pseudo-JT (PJT) coupling of the $G_{3/2}$ and $E_{5/2}$ manifolds. Depending on the signs of a and α, there is constructive or destructive interference of the electrostatic and relativistic JT couplings.

For sufficiently large values of the SO splitting 3Δ, the $G_{3/2}$ manifold (with eigenvalues $E_{T_2} - \Delta$) can be considered to be approximately decoupled from the $E_{5/2}$ manifold (with eigenvalue $E_{T_2} + 2\Delta$) [52]. In this approximation, the $^2T_2 \times t_2$ JT Hamiltonian is reduced to a 4×4 matrix

$$\widetilde{\mathcal{H}}^{(1)}[G_{3/2} \times t_2] = (E_{T_2} - \Delta)\mathbf{1}_4 + i\tilde{a}_1 \begin{pmatrix} 0 & -Q_+ & 0 & Q_z \\ Q_- & 0 & -Q_z & 0 \\ 0 & Q_z & 0 & Q_- \\ -Q_z & 0 & -Q_+ & 0 \end{pmatrix}. \tag{47}$$

The eigenvalues of this vibronic matrix are

$$V_1 = V_2 = E_{T_2} - \Delta - |\tilde{a}_1|R \tag{48a}$$

$$V_3 = V_4 = E_{T_2} - \Delta + |\tilde{a}_1|R \tag{48b}$$

where

$$R = (Q_x^2 + Q_y^2 + Q_z^2)^{\frac{1}{2}}. \tag{48c}$$

The adiabatic potentials (48) are doubly degenerate (Kramers degeneracy) and represent a double cone in four-dimensional space (the energies as a function of three nuclear coordinates).

The analysis for a ^2E state, which transforms as $G_{3/2}$ in T_d', is analogous and has been discussed in Ref. [27]. For brevity, we consider here only the t_2 vibrational mode. The Hamiltonian matrix in the linear approximation reads [27]

$$\mathcal{H}^{(1)}[^2E \times t_2] = E_E\mathbf{1}_4 + i\gamma \begin{pmatrix} 0 & Q_z & Q_- & 0 \\ -Q_z & 0 & 0 & -Q_- \\ -Q_+ & 0 & 0 & Q_z \\ 0 & Q_+ & -Q_z & 0 \end{pmatrix} \tag{49}$$

As discussed in Section 3.1, the zeroth-order SO splitting vanishes for a ^2E state in tetrahedral symmetry. Moreover, the linear electrostatic $^2E \times t_2$ JT coupling constant is zero by symmetry (see Eq. (23a)). The linear JT coupling constant γ in Eq. (49) is thus of purely relativistic origin. The eigenvalues of the vibronic matrix (49) are given by Eq. (48), with $|\tilde{a}_1|$ replaced by $|\gamma|$.

The $^2T_2 \times e$ and $^2E \times e$ JT Hamiltonians of tetrahedral systems are not discussed in detail in this synopsis for brevity. The results can be found in Refs. [27, 28]. The $^2E \times e$ case in tetrahedral symmetry is remarkable. As is well known, the zeroth-order SO splitting is zero for a ^2E state in tetrahedral symmetry [4–6, 10]. A detailed analysis reveals that the SO coupling within a ^2E state vanishes in any order of the normal mode of e symmetry. The $^2E \times e$ JT effect in tetrahedral systems is thus strictly unaffected by SO coupling.

As is well known, the electrostatic $^2T_2 \times (t_2 + e)$ and $^2E \times (t_2 + e)$ JT Hamiltonians up to second order are the same in tetrahedral and cubic systems, apart from the obvious additional restrictions due to inversion symmetry [4–11]. The relativistic JT forces, on the other hand, are not identical in tetrahedral and cubic systems. A detailed analysis reveals that the $^2T_2 \times e$ JT coupling has electrostatic as well as relativistic contributions in tetrahedral systems [28]. In octahedral and cubic systems, on the other hand, the linear relativistic $^2T_{2g} \times e_g$ coupling parameter is zero by symmetry [29]. This fact reveals that the symmetry selection rules for the SO operator differ from those for the electrostatic Hamiltonian in a subtle manner.

3.4. Application: The $^2T_2 \times t_2$ Jahn-Teller effect in Sb_4^+

Recent *ab initio* calculations of the matrix elements of the Breit-Pauli operator with nonrelativistic CASSCF wave functions and diagonalization of the SO-CI matrix have established the zeroth-order SO splittings of the T_2 state and have confirmed, moreover, the existence of substantial linear relativistic JT couplings for the heavier group-V tetramers [57].

Herein, we restrict our attention to JT and SO coupling in Sb_4^+, referring to Ref. [58] for a comparative discussion of the photoelectron spectra of P_4, As_4, Sb_4 and Bi_4. The electrostatic as well as relativistic JT couplings of the e mode in the $^2T_2$ state are rather weak and have little impact on the JT spectra [58]. For clarity, we therefore discuss the pure $T_2 \times t_2$ effect in Sb_4^+.

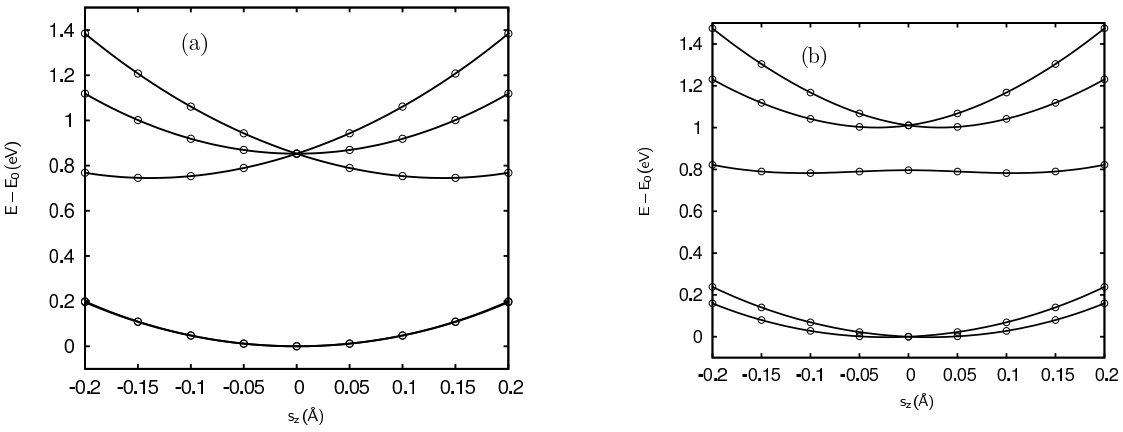

Figure 3. Electrostatic (a) and relativistic (b) PE surfaces of the electronic ^2E ground state and the $^2T_2$ first excited state for Sb_4^+ (circles: *ab initio* data; solid lines: fit)

.

Cuts of the PE surfaces of the ^2E and $^2T_2$ states of Sb_4^+ along the t_2 symmetry coordinate s_z, obtained without (a) and with SO coupling (b), are shown in Fig. 3. Fig. 3a reveals the very strong electrostatic $T_2 \times t_2$ JT splitting in the $^2T_2$ state upon distortion in the t_2 mode. Fig. 3b

shows the PE functions obtained with inclusion of SO coupling. It illustrates the zeroth-order SO splitting of the $^2T_2$ state into $G_{3/2}$ and $E_{5/2}$ states. Moreover, it can be seen that the JT splitting of the $G_{3/2}$ state in (b) is significantly weaker than the JT splitting of the nonrelativistic $^2T_2$ state in (a). This feature reflects the destructive interference between a and α in Eq. (46b) ($a/\omega_{t_2} = 3.2, \alpha/\omega_{t_2} = -0.58$). Moreover, it is seen that the PE functions of the ^2E state in Fig. 3b exhibit a splitting as a function of s_z, which is the signature of the relativistic $^2E \times t_2$ JT coupling ($\gamma/\omega_e = 0.02$).

The photoelectron spectrum of the $^2T_2$ state of Sb_4^+, calculated in the nonrelativistic approximation, is displayed in Fig. 4. The sharp lines in Fig. 4 correspond to a resolution of 0.5 meV (which is determined by the total propagation time of the calculation). The envelope in Fig. 4 represents a "low-resolution spectrum", which was obtained from the high-resolution spectrum by convolution with a Gaussian of 15 meV full width at half maximum [58]. The photoelectron band of the $^2T_2$ state of Sb_4^+ is characteristic for a very strong $^2T_2 \times t_2$ JT effect ($a/\omega_{t_2} = 3.2$). The energy levels as well as the intensities are highly irregular, reflecting the pronounced anharmonicity of the adiabatic PE surfaces and strong nonadiabatic couplings. The low-resolution envelope, on the other hand, exhibits a quasi-regular progression, see Fig. 4.

The $^2T_2$ photoelectron spectrum obtained with inclusion of zeroth-order SO splitting ($\Delta = -71.45$ meV) is shown in Fig. 5a. The photoelectron band splits into two sub-bands with a separation of approximately 3Δ (0.21 eV). In addition, we observe a significant reduction of the extension of the quasi-progression in the t_2 mode, which reflects the quenching of the $T_2 \times t_2$ JT coupling by the zeroth-order SO splitting.

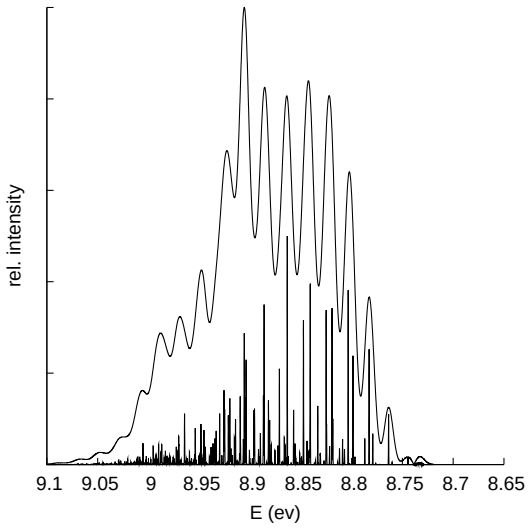

Figure 4. $^2T_2 \times t_2$ JT spectrum of Sb_4^+

.

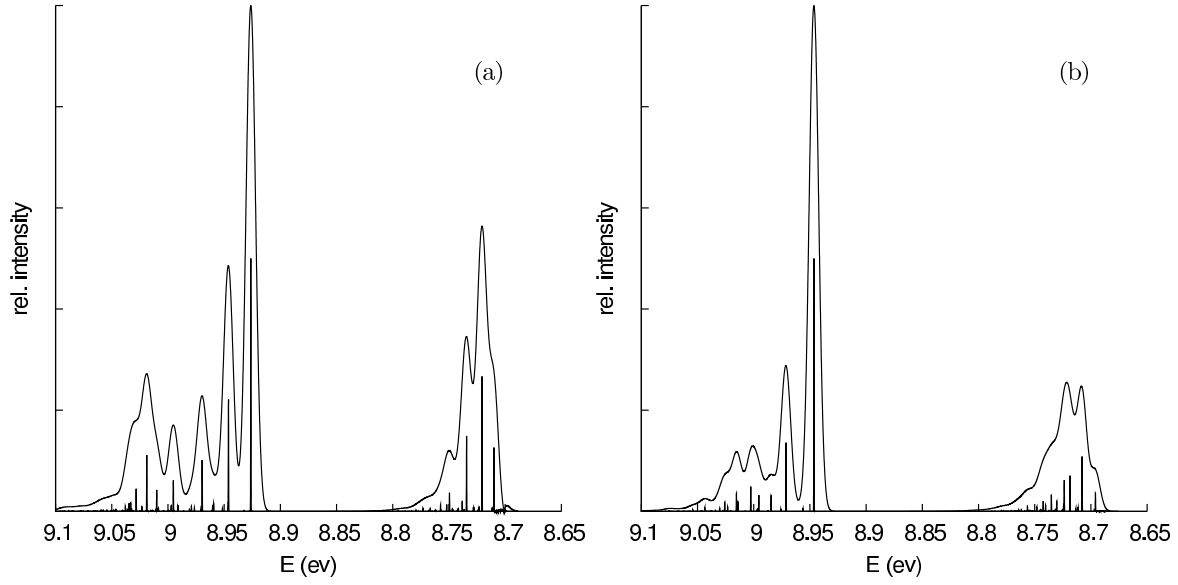

Figure 5. ${}^2T_2 \times t_2$ JT spectrum of Sb_4^+ including zeroth-order (a) and zeroth plus first-order (b) SO coupling

.

When the linear relativistic SO coupling constant α is additionally included, the ${}^2T_2$ photoelectron band displayed in Fig. 5b is obtained. It can be seen that the quasi-progression in the upper ($G_{3/2}$) state is shorter than in Fig. 5a, while the quasi-progression in the lower ($E_{5/2}$) state is more extended than in Fig. 5a. These features reflect the destructive and constructive interference in $\tilde{a}_1$ and $\tilde{a}_2$, respectively (see Eq. (46b, c)). The inclusion of the linear relativistic JT couplings thus is necessary for an accurate prediction of the vibronic structure of the photoelectron spectrum of Sb_4. As expected, these effects are even larger in the photoelectron spectrum of Bi_4 [58].

The available experimental photoelectron spectra of P_4, As_4 and Sb_4 are strongly broadened due to the high temperature of the clusters [53–56]. As a result, the existing photoelectron spectrum of Sb_4 is structureless [55, 56]. A high-resolution photoelectron spectrum of cold tetrahedral Sb_4 clusters would be of great interest for the future development of JT theory.

4. Summary and outlook

In this synopsis, we sketched the concepts of a systematic extension of JT theory beyond the standard model. The latter has been the paradigm for the analysis of static and dynamic JT effects in Physics and Chemistry since many decades. The motivation for a substantial extension of JT theory arises from modern computational electronic-structure theory, which can provide an essentially unlimited amount of PE data for JT systems, including an accurate description of SO coupling effects. The traditional expansions of the electrostatic PEs up to second order and the SO coupling energies up to zeroth order are insufficient for an accurate modeling of the *ab initio* data.

For the electrostatic (spin-less) Hamiltonian, we have summarized herein the high-order expansions of the two most generic and common JT Hamiltonians: the $E \times e$ Hamiltonian in C_{3v} symmetry and the $T_2 \times t_2$ Hamiltonian in T_d symmetry. Since C_{3v} is a subgroup of C_{6h}, T_d, and O_h, the $E \times e$ master JT Hamiltonian is also valid for these groups. Likewise, T_d is a subgroup of O_h. Therefore, the $T_2 \times t_2$ master JT Hamiltonian applies also in cubic symmetry. The conventional Taylor expansion of the electronic Hamiltonian has been replaced by an expansion

in invariant polynomials, employing the powerful tools of invariant theory [25, 41]. Invariant theory allows the construction of JT expansions up to arbitrary order. Since the $E \times e$ and $T_2 \times t_2$ JT Hamiltonians are symmetric in the electronic and nuclear vector spaces, Weyl's polarization method can be employed and results in an elegant construction method of high-order JT Hamiltonians.

It has recently been shown by *ab initio* electronic-structure calculations for representative JT systems (e.g. NH_3^+ [20], NO_3 [19], CH_4^+ [23, 24] and transition-metal trifluorides [21, 22]) that for strong JT effects involving bending modes the expansion of the electrostatic potential up to second order is generally insufficient. Intramolecular collisions of the ligand atoms lead to pronounced positive anharmonicities. As a result, expansions of the PEs of the bending modes at least up to sixth order are a necessity.

The second restriction of the standard model of JT theory is the approximation of the SO coupling operator in zeroth-order of the normal-mode Taylor expansion. Recently, the theory of SO coupling in JT systems was extended beyond the standard model by the Taylor expansion of the Breit-Pauli SO operator up to first order in normal-mode displacements for the common spin double groups (trigonal, tetragonal, tetrahedral and cubic systems) [26–30]. If considered necessary, the expansion of the Breit-Pauli operator could be extended to include second-order terms. Since a nonrelativistic spin-orbital electronic basis was employed, the SO coupling appears as a perturbation of the nonrelativistic electronic Hamiltonian. The contributions of the electrostatic (Coulombic) interactions and the electrodynamic (current-induced) contributions are thus explicitly exhibited for each JT coupling constant. The different scaling of the electrostatic and relativistic interactions with the nuclear charge Z of heavy elements is thus transparent. Moreover, the SO-induced JT couplings are *a priori* obtained in a diabatic form. The diabatic basis of the nonrelativistic Hamiltonian is sufficient; no additional diabatization procedure is necessary. From a practical point of view, it is helpful that the matrix elements of the full (two-electron) Breit-Pauli operator with nonrelativistic CASSCF wave functions are efficiently implemented in several of the widely available electronic-structure codes (e.g. GAMESS, MOLPRO, MOLCAS).

For molecules, molecular complexes and crystals containing very heavy elements, the so-called two-step approach to relativistic electronic-structure (treating electron correlation first at the electrostatic level, followed by inclusion of SO-coupling effects by the diagonalization of the Breit-Pauli operator) may become slowly convergent and therefore inefficient [62]. In this case, it may be preferable to formulate the JT theory by employing a two-component electronic spinor basis (provided, e.g., by the ZORA, Douglas-Kroll-Hess or exact two-component (X2C) methods [32, 63]). A quasi-diabatic electronic basis has then to be defined at the relativistic level. The methods of invariant theory outlined in Section 2 may then be employed in the framework of the spin double groups.

References

[1] Jahn H A and Teller E 1937 *Proc. Roy. Soc. (London)* A **161** 220
[2] Renner E 1934 *Z. Physik* **92** 172
[3] Longuet-Higgins H C 1961 *Advances in Spectroscopy* vol 2, ed H W Thompson (New York: Interscience) p 429
[4] Sturge M D 1967 *Solid State Phys.* **20** 91
[5] Englman R 1972 *The Jahn-Teller Effect* (New York: Wiley)
[6] Bersuker I B and Polinger V Z 1989 *Vibronic Interactions in Molecules and Crystals* (Heidelberg: Springer)
[7] O'Brien M C M and Chancey C C 1993 *Am. J. Phys.* **61** 688
[8] Bersuker I B 2001 *Chem. Rev.* **101** 1067
[9] Applegate B E, Barckholtz and Miller T A 2003 *Chem. Soc. Rev.* **32** 38
[10] Bersuker I B 2006 *The Jahn-Teller Effect* (Cambridge University Press)
[11] Köppel H, Yarkony D R and Barentzen H (eds.) 2009 *The Jahn-Teller Effect* (Heidelberg: Springer)

[12] We follow the convention that uses the capital letters for the symmetry labels of electronic states and lowercase letters for the symmetry labels of vibrational modes.
[13] García-Fernández P, Bersuker I B, Aramburu J A, Barriuso M T and Moreno M 2005 *Phys. Rev.* B **71** 184117
[14] Marenich A V and Boggs J E 2005 *Chem. Phys. Lett.* **404** 351
[15] Hauser A W, Callegari C, Soldán P and Ernst W E 2010 *Chem. Phys.* **375** 73
[16] Hauser A W, Auböck G, Callegari C and Ernst W E 2010 *J. Chem. Phys.* **132** 164310
[17] Viel A and Eisfeld W 2004 *J. Chem. Phys.* **120** 4603
[18] Marenich A V and Boggs J E 2005 *J. Chem. Phys.* **122** 024308
[19] Faraji S, Köppel H, Eisfeld W and Mahapatra S 2008 *Chem. Phys.* **347** 110
[20] Viel A, Eisfeld W, Neumann S, Domcke W and Manthe U 2006 *J. Chem. Phys.* **124** 214306
[21] Mondal P, Opalka D, Poluyanov L V and Domcke W 2011 *Chem. Phys.* **387** 56
[22] Mondal P, Opalka D, Poluyanov L V and Domcke W 2012 *J. Chem. Phys.* **136** 084308
[23] Opalka D and Domcke W 2010 *J. Chem. Phys.* **132** 154108
[24] Opalka D and Domcke W 2010 *Chem. Phys. Lett.* **494** 134
[25] Derksen H and Kemper G 2002 *Computational Invariant Theory* (New York: Springer)
[26] Domcke W, Mishra S and Poluyanov L V 2006 *Chem. Phys.* **322** 405
[27] Poluyanov L V and Domcke W 2008 *J. Chem. Phys.* **129** 224102
[28] Poluyanov L V and Domcke W 2010 *Chem. Phys.* **374** 86
[29] Poluyanov L V and Domcke W 2012 *J. Chem. Phys.* **137** 114101
[30] Poluyanov L V and Domcke W 2012 *Chem. Phys.* **407** 1
[31] Bethe H A and Salpeter E E 1957 *Quantum Mechanics for One and Two Electron Atoms* (Berlin: Springer)
[32] Dyall K G and Faegri K 2007 *Relativistic Quantum Chemistry* (Oxford University Press)
[33] Bunker P R and Jensen P 1998 *Molecular Symmetry and Spectroscopy (second edition)* (Ottawa: NRC Research Press)
[34] Collins M A and Parsons D F 1993 *J. Chem. Phys.* **99** 6756
[35] Braams B J and Bowman J M 2009 *Int. Rev. Phys. Chem.* **28** 577
[36] Hilbert D 1890 *Math. Ann.* **36** 473
[37] Noether E 1915 *Math. Ann.* **77** 89
[38] Lichten W 1967 *Phys. Rev.* **164** 131
[39] Smith F T 1969 *Phys. Rev.* **179** 111
[40] Pacher T, Cederbaum L S and Köppel H 1993 *Adv. Chem. Phys.* **84** 293
[41] Weyl H 1946 *The Classical Groups. Their Invariants and Representations* (Princeton: Princeton University Press)
[42] Ascher E and Gay D 1985 *J. Phys.* A: Math. Gen. **18** 397
[43] Meiswinkel R and Köppel H 1993 *Chem. Phys. Lett.* **201** 449
[44] Werner H J, Knowles P J, et al., MOLPRO, Version 2006.1 and 2008, see http://www.molpro.net
[45] Hamermesh M 1962 *Group Theory and its Application to Physical Problems* (Reading: Addison-Wesley)
[46] Balasubramanian K 1997 *Relativistic Effects in Chemistry,* Part A (New York: Wiley)
[47] Chau F T and Karlsson L 1977 *Phys. Scripta* **16** 258
[48] We use symbols $E_{1/2}$, $E_{5/2}$, $G_{3/2}$ of Hamermesh for the irreducible representations of T_d' and O_h'. In the solid-state literature, these representations are denoted as Γ_6, Γ_7, Γ_8.
[49] Wigner E 1959 *Group Theory* (New York: Academic Press)
[50] Jahn H A 1938 *Proc. Roy. Soc. (London)* A **164** 117
[51] Ceulemans A 1987 *J. Chem. Phys.* **87** 5374
[52] Moffitt W and Thorson W 1957 *Phys. Rev.* **108** 1251
[53] Elbel S, Kudnig J, Grodzicki M and Lempka H J 1984 *Chem. Phys. Lett.* **109** 312
[54] Dyke J M, Morris A and Stevens J C H 1986 *Chem. Phys.* **102** 29
[55] Wang L-S, Niu B, Lee Y T, Shirley D A, Ghelichkhani E and Grant E R 1990 *J. Chem. Phys.* **93** 6318
[56] Wang L-S, Niu B, Lee Y T, Shirley D A, Ghelichkhani E and Grant E R 1990 *J. Chem. Phys.* **93** 6327
[57] Opalka D, Segado M, Poluyanov L V and Domcke W 2010 *Phys. Rev.* A **81** 042501
[58] Opalka D, Poluyanov L V and Domcke W 2011 *J. Chem. Phys.* **135** 104108
[59] Heller E J 1981 *Acc. Chem. Res.* **14** 368
[60] Schinke R 1993 *Photodissociation Dynamics* (Cambridge, UK: Cambridge University Press)
[61] Tal-Ezer H and Kosloff R 1984 *J. Chem. Phys.* **81** 3967
[62] Fleig T 2012 *Chem. Phys.* **395** 2
[63] Liu W 2010 *Mol. Phys.* **108** 1679